

## NEW MODEL PREDICTING FLOW CURVES IN WIDE RANGE OF THERMOMECHANICAL CONDITIONS OF 38MnVS6 STEEL

OPĚLA Petr<sup>1</sup>, SCHINDLER Ivo<sup>1</sup>, KAWULOK Petr<sup>1</sup>, VANČURA Filip<sup>2</sup>,  
KAWULOK Rostislav<sup>1</sup>, RUSZ Stanislav<sup>1</sup>

<sup>1</sup>VSB - Technical University of Ostrava, Czech Republic, EU  
[petr.opela@vsb.cz](mailto:petr.opela@vsb.cz), [ivo.schindler@vsb.cz](mailto:ivo.schindler@vsb.cz), [petr.kawulok@vsb.cz](mailto:petr.kawulok@vsb.cz), [rostislav.kawulok@vsb.cz](mailto:rostislav.kawulok@vsb.cz),  
[stanislav.rusz2@vsb.cz](mailto:stanislav.rusz2@vsb.cz)

<sup>2</sup>Kovárna VIVA a.s., Zlín, Czech Republic, EU, [filip.vancura@viva.cz](mailto:filip.vancura@viva.cz)

### Abstract

Prediction capability of a newly derived hot flow stress model is demonstrated on experimental flow curves of steel 38MnVS6. These flow curves were also described by the commonly used equations like Cingara & McQueen, JMAK or Hensel-Spittel. Graphical and statistical comparison proved that flow curve prediction by the newly derived model leads to the best fit with the experimental data. An advantage of the new model was discovered especially in case of the flow curves acquired in very broad range of thermomechanical conditions when shapes of these curves may very differ.

**Keywords:** Hot compression flow curves, flow curve characteristic points, hot flow stress model

### 1. INTRODUCTION

In recent years, a lot of researches were focused to develop a suitable model to precisely predict flow curves of numerous types of materials under various ranges of thermomechanical conditions [1]. Many of these models find their utilization for various materials at tested conditions. Nevertheless, a recent research revealed that flow curves acquired in a wide range of thermomechanical conditions make limitation in prediction capabilities in case of all these models. Flow curves may have very different shape in a wide range of deformation temperature and strain rate. This phenomenon is especially significant in the after-the-peak-point area, which can be deeply influenced by various dynamic recrystallization development [2]. So, the main aim of this paper is to introduce a new model which will be able to predict flow curves in a wide range of thermomechanical conditions.

### 2. EXPERIMENT

Cylindrical compression-test specimens of steel 38MnVS6 with the diameter of 10 mm and the height of 15 mm were prepared and set of twenty uniaxial hot compression tests were performed on the Hot Deformation Simulator HDS-20 at VSB-TU Ostrava whose testing module Hydrawedge II [3] enables to achieve the nominal strain rate up to 100 s<sup>-1</sup> [4]. The deformation temperature range of 1280 °C - 1200 °C - 1100 °C - 1000 °C - 850 °C and the strain rate range of 0.1 s<sup>-1</sup> - 1 s<sup>-1</sup> - 10 s<sup>-1</sup> - 100 s<sup>-1</sup> were chosen to cover a wide spectrum of flow curve types to create a suitable hot flow stress model. Each sample was firstly preheated by the 5 °C·s<sup>-1</sup> up to the temperature of 1250 °C with the following dwell of 30 s. After that was further preheated by the same rate up to the temperature of 1280 °C with the following dwell of 10 s. Each sample was after this two-stage preheating cooled down to the deformation temperature and then deformed by the uniaxial compression with the maximum height-true strain of 1.0.

### 3. RESULTS AND DISCUSSION

#### 3.1. Characteristic points of the flow curves

Prediction of the peak and steady-state points is an important step to assembly accurate flows tress models.

The well-known Garofalo equation was rewritten to predict the peak stress values  $\sigma_p$  (MPa) of the investigated steel 38MnVS6. So, this equation takes the following particular form [5]:

$$\sigma_p = \frac{1}{0.0086} \cdot \arg \sinh 4.6 \sqrt{\frac{Z}{3 \cdot 10^{12}}} \quad (1)$$

Next power-law function was used to calculate the peak strain values  $e_p$  (-) [5]:

$$e_p = 0.0025 \cdot Z^{0.17} \quad (2)$$

The Zener-Hollomon parameter  $Z$  (s<sup>-1</sup>) has the known form [6]:

$$Z = \dot{\epsilon} \cdot \exp\left(\frac{Q}{R \cdot T}\right) \quad (3)$$

The variable  $\dot{\epsilon}$  (s<sup>-1</sup>) is the strain rate,  $T$  (K) is the deformation temperature and  $R$  (8.314 J·K<sup>-1</sup>·mol<sup>-1</sup>) is the universal gas constant. The activation energy at hot forming  $Q$  (J·mol<sup>-1</sup>) is widely used material characteristic in case of the flow curve description. The value of the  $Q$  and other material constants in the above mentioned equations were estimated by the special interactive software ENERGY 4.0, working on the principle of partial linear regressions [7]. The resulting value of the  $Q$  was in case of the investigated steel estimated as 316 kJ·mol<sup>-1</sup>. The steady-state stress  $\sigma_{ss}$  (MPa) was then calculated on basis of linear estimation on the peak stress values as follows [5]:

$$\sigma_{ss} = 0.89 \cdot \sigma_p \quad (4)$$

### 3.2. Flow curve modeling up to the peak point

The Cingara and McQueen is widely used equation to describe flow curve up to the peak point [8]. The particular expression of this model in case of the steel 38MnVS6 is following:

$$\sigma = \sigma_p \cdot \left[ \frac{e}{e_p} \cdot \exp\left(1 - \frac{e}{e_p}\right) \right]^{(0.36 \cdot \dot{\epsilon} + 4.18) Z^{(-0.00068 \cdot \dot{\epsilon} - 0.092)}} \quad (5)$$

where  $\sigma$  (MPa) and  $e$  (-) are the flow stress and strain up to the peak point and  $\sigma_p$  (MPa) (Eq. 1),  $e_p$  (-) (Eq. 2) are the peak stress and strain, respectively.

### 3.3. Flow curve modeling beyond the peak point

One of the most used equations to model flow curves beyond the peak point (JMAK) is based on the Avrami kinetics of recrystallization. The JMAK formula can be established as in [9]. The particular expression of this model in case of the steel 38MnVS6 is following:

$$\sigma = \sigma_{ss} + (\sigma_p - \sigma_{ss}) \cdot \exp\left[-1.2 \cdot \left(\frac{e - e_p}{e_p}\right)^{0.98}\right] \quad (6)$$

where  $\sigma$  (MPa) and  $e$  (-) are the flow stress and strain beyond the peak point and  $e_p$  (-) (Eq. 2),  $\sigma_p$  (MPa) (Eq. 1),  $\sigma_{ss}$  (MPa) (Eq. 4) are the peak strain, peak and steady-state stress, respectively.

### 3.4. Flow curve modeling in entire range of strains

Often used model enabling flow stress description in wide range of strains is the phenomenological Hensel-Spittel formula [10]. In case of the steel 38MnVS6 take this formula particular form:

$$\sigma = 1394872 \cdot \exp(-0.0027 \cdot t) \cdot t^{-0.92} \cdot e^{0.19} \cdot \exp\left(\frac{-0.0054}{e}\right) \cdot (1 + e)^{-0.00058t} \cdot \exp(0.032 \cdot e) \cdot \dot{\epsilon}^{-0.14} \cdot \dot{\epsilon}^{0.00029t} \quad (7)$$

where  $\sigma$  (MPa) represents the flow stress in whole range of examined strains, except  $e$  smaller than ca 0.04 and  $e$  (-) is the strain of the range from ca 0.04 and higher. The variables  $\dot{\epsilon}$  (s<sup>-1</sup>) and  $t$  (°C) are the strain rate and deformation temperature, respectively. Material constants of the Eq. (7) were achieved by nonlinear regression analysis in the statistical software UNISTAT 5.6 [11] knowing their rough estimates from the previous modeling.

### 3.5. New hot flow stress description

The flow curves of the investigated steel were described up to the peak point by the following newly derived equation:

$$\sigma_1 = A \cdot \left\{ \frac{e}{e_p} \cdot \left[ 1 + \sinh \left( 1 - \frac{e}{e_p} \right) \right] \right\}^{a_1 \cdot Z^{b_1}} \cdot \dot{\epsilon}^{\left( \frac{B-C}{T} \right)} \cdot \exp(-D \cdot T) \quad (8)$$

Where  $\sigma_1$  (MPa) and  $e$  (-) represent the flow stress and strain up to the peak,  $e_p$  (-) (Eq. 2) is the peak strain,  $\dot{\epsilon}$  (s<sup>-1</sup>) and  $T$  (K) are the strain rate and deformation temperature, respectively. Rough estimation of the material constants  $A$  (MPa·s),  $B$  (-),  $C$  (K),  $D$  (K<sup>-1</sup>),  $a_1$  (s) and  $b_1$  (-) can be obtained by regression analysis. The first step is to obtain the constants  $A$ ,  $B$ ,  $C$  and  $D$ . The one important condition must be taken into account - the  $\sigma_1$  must be equal to the peak stress  $\sigma_p$  when the strain is equal to the peak strain  $e_p$ . Then Eq. (8) could be expressed as:

$$\sigma_p = A \cdot \dot{\epsilon}^{\left( \frac{B-C}{T} \right)} \cdot \exp(-D \cdot T) \quad (9)$$

where  $\sigma_p$  (MPa) represents the experimental peak stress. The slope of the line  $a = B - C / T$  and the intercept  $b = -D \cdot T + \ln A$  can be obtained at each temperature by plotting the  $\ln \sigma_p$  vs.  $\ln \dot{\epsilon}$ . Then, from the slope and intercept of the Eq. (10) can be obtained constants  $C$  and  $B$ . Constants  $D$  and  $A$  is possible to obtain similarly from Eq. (11):

$$a = -C \cdot \frac{1}{T} + B \quad (10)$$

$$b = -D \cdot T + \ln A \quad (11)$$

When the material constants  $A$ ,  $B$ ,  $C$  and  $D$  are known, the strain hardening exponent of the Eq. (8) should be substituted as  $n_1$  (-):

$$n_1 = a_1 \cdot Z^{b_1} \quad (12)$$

Then can be experimental values of the hardening exponent  $n_1$  estimated for each flow curve by plotting the  $\ln(\sigma_1 / \sigma_p)$  vs.  $\ln(e / e_p) + \ln[1 + \sinh(1 - e / e_p)]$ . The  $\sigma_p$  is given by the Eq. (9).

After that, material constants  $a_1$  and  $b_1$  can be gained from the logarithmic form of the Eq. (12), i.e.  $\ln n_1$  vs.  $\ln Z$ . In order to achieve the best fit of the predicted curves with experimental ones, it is recommended to utilize nonlinear regression analysis of the complete Eq. (8) with the above calculated material constants as rough estimations. In case of the studied steel 38MnVS6 was utilized the statistic software UNISTAT 5.6. By this way refined constants are shown in **Table 1**.

Description of the experimental flow curves beyond the peak point was done by another newly derived formula:

$$\sigma_2 = \sigma_{ss} + (\sigma_p - \sigma_{ss}) \cdot \left[ \frac{e}{e_p} \cdot \exp \left( 1 - \frac{e}{e_p} \right) \right]^{a_2 \cdot Z^{b_2}} \quad (13)$$

where  $\sigma_2$  (MPa) and  $e$  (-) are the flow stress and strain beyond the peak point and  $e_p$  (-) (Eq. 2),  $\sigma_p$  (MPa) (Eq. 9),  $\sigma_{ss}$  (MPa) (Eq. 4) are the peak strain, peak and steady-state stress, respectively. It is important to note, that the value of the  $\sigma_{ss}$  must be in the Eq. (4) related to the  $\sigma_p$  from the Eq. (9), not from the Eq. (1). Rough estimations of the material constants  $a_2$  (s) and  $b_2$  (-) can be obtained by introducing the softening exponent  $n_2$  (-):

$$n_2 = a_2 \cdot Z^{b_2} \quad (14)$$

The values of  $n_2$  are possible to obtain for each curve from the linear form of the Eq. (13), taking into account Eq. (14), i.e.  $\ln[(\sigma_2 - \sigma_{ss}) / (\sigma_p - \sigma_{ss})]$  vs.  $1 - e / e_p + \ln(e / e_p)$ . Then can be material constants  $a_2$  and  $b_2$  achieved by plotting the  $\ln n_2$  vs.  $\ln Z$ .

The rough estimations of the material constants  $a_2$  and  $b_2$  were then put in to the Eq. (13) and subjected, as in previous case, to the nonlinear regression analysis in the UNISTAT 5.6. By this way advanced constants are also shown in **Table 1**.

The complete form of the newly derived model can be then written as:

$$\sigma = \begin{cases} \sigma_1 \text{ (8)} & \text{for } e \leq e_p \\ \sigma_2 \text{ (13)} & \text{for } e \geq e_p \end{cases} \quad (15)$$

**Table 1** Material constants of the newly derived model (15)

A (MPa·s)	B (-)	C (K)	D (K <sup>-1</sup> )	a <sub>1</sub> (s)	b <sub>1</sub> (-)	a <sub>2</sub> (s)	b <sub>2</sub> (-)
13660	0.44	378	0.0037	7.08	-0.11	12691	-0.23

### 3.6. Comparison of the experimental and predicted flow curves

Graphical and statistical methods were used in order to adequately compare the experimental flow curves with the predicted one. The graphical comparison is shown in **Figure 1**. Cingara & McQueen formula (5) provides good prediction of the flow curves up to the peak point. Nevertheless, the perfect match with the experimental curves up to the peak was achieved by the newly derived model (15), which is also confirmed in **Figure 2** by the Root Mean Square Error RMSE (MPa) [12]:

$$\text{RMSE} = \sqrt{\frac{1}{n} \cdot \sum_{i=1}^n (\sigma_i - \sigma(e_i))^2} \quad (16)$$

In Eq. (16),  $n$  (-) represent the number of data points involved in calculations,  $\sigma_i$  (MPa) is the target value and  $\sigma(e_i)$  (MPa) is the model output, i.e. experimental flow stresses and predicted one, respectively.

Hensel-Spittel model (7) can also describe the flow curve up to the peak, but its prediction capability exhibits less reliability (see **Figures 1** and **2**). Moreover, it is obvious that the Hensel-Spittel model lacks an ability to correctly describe the flow curves with the significant peak point followed by the rapid flow decrease into the steady-state area. This is because of its purely phenomenological flow curve description without any physical base taking into account the significant DRX influence. Thus, the Hensel-Spittel equation is not even appropriate to use for flow curve description beyond the peak point if significant DRX softening occurs.

JMAK model (6) is derived to describe the after-the-peak-point region. It is obvious that its prediction capability in this area is better than ability of the Hensel-Spittel equation (7). However, the newly derived model (15) shows even much better fit with the experimental curves, which is also confirmed by the graphical and statistical comparison (**Figure 1** and **Figure 2**).

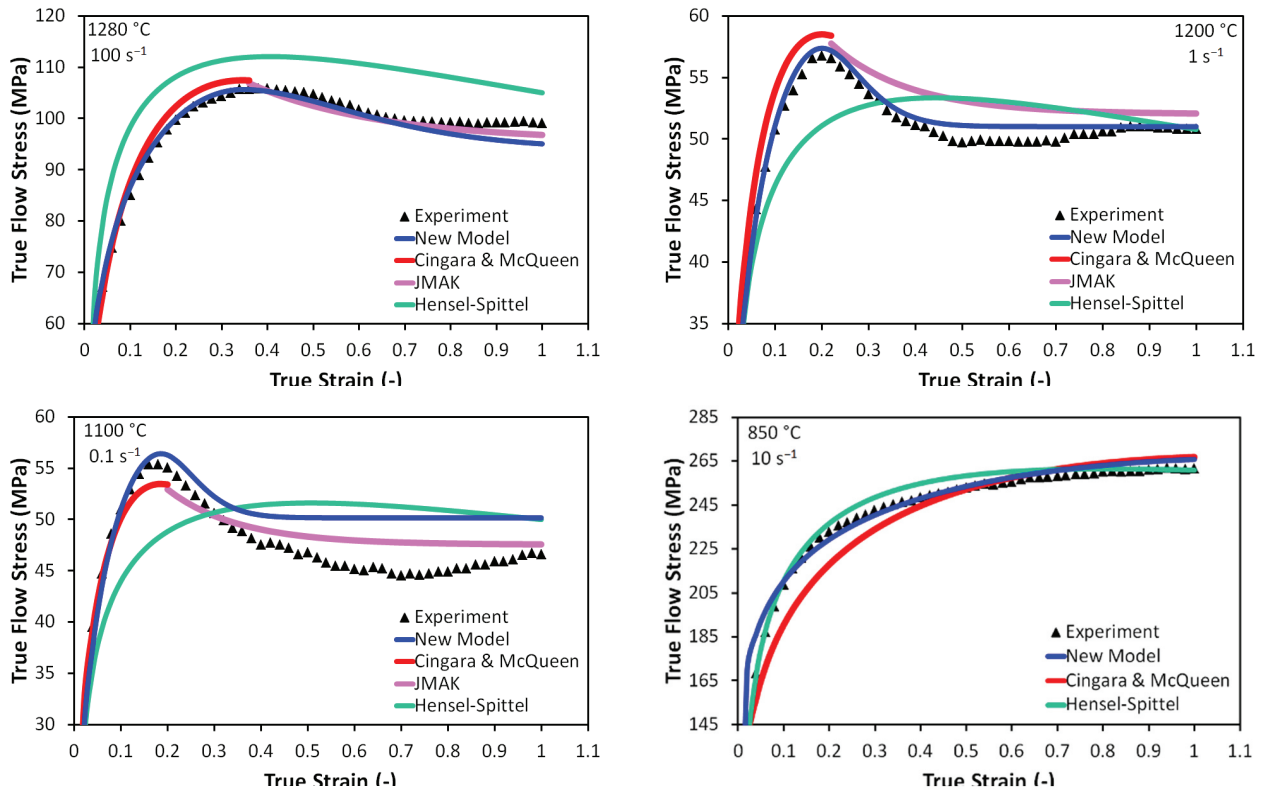


**Figure 1** Graphical comparison of the selected experimental and predicted flow curves

The main advantage of the newly derived model (15) lies in its capability to describe flow curves beyond the peak point in wide range of thermomechanical conditions all at once. This new model can thus describe flow curves with significant influence of DRX when after what is the peak point reached flow curve rapidly decrease and then steady-state follows. The new model is then simultaneously able to describe flow curves without distinct DRX influence and steady-state area. These affirmations are confirmed by the **Figure 1** and the best fit with the experimental curves is substantiated by the RMSE in **Figure 2**.

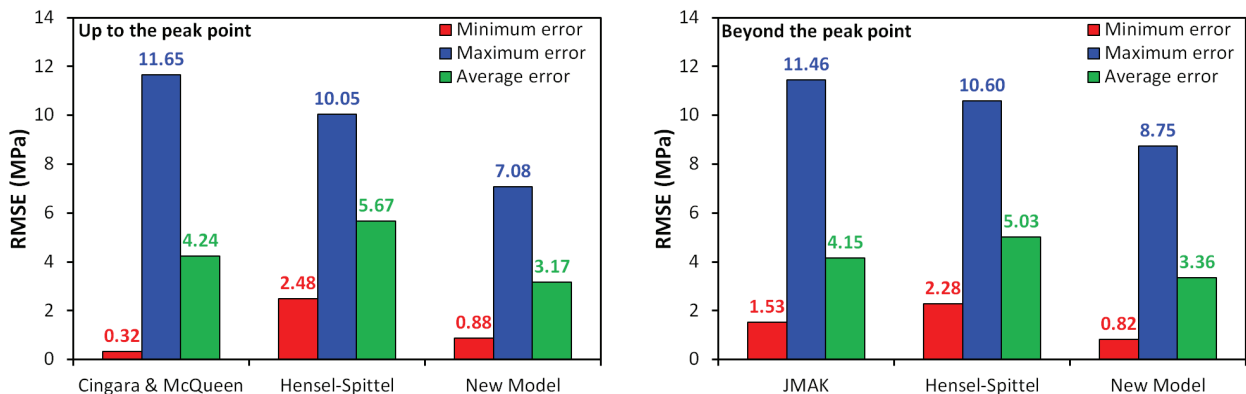


**Figure 2** Statistical comparison of the examined models

#### 4. CONCLUSION

In this research, uniaxial hot compression test of the steel 38MnVS6 was performed in the wide temperature range of 850 °C - 1280 °C and the strain rate range of 0.1 s<sup>-1</sup> - 100 s<sup>-1</sup>. The experimental flow curves were

described up to the peak point by the widely used Cingara and McQueen equation and beyond the peak by the Johnson-Mehl-Avrami-Kolmogorov (JMAK) model. The commonly used phenomenological Hensel-Spittel model was then used to describe entire strain range of the examined flow curves. A brand new model was derived to describe flow curves up to the peak point and also beyond them. Graphical and statistical comparisons have showed a higher suitability of this derived model. The main contribution of the new model is possibility to describe flow curves with significant influence of DRX softening and presence of steady-state area together with curves which are free of these features.

## ACKNOWLEDGEMENTS

***This paper was created on the Faculty of Metallurgy and Materials Engineering in the Project No. LO1203 "Regional Materials Science and Technology Centre - Feasibility Program" and in within the frame of the Student Grant Competition SP2016/66 funded by Ministry of Education, Youth and Sports of the Czech Republic.***

## REFERENCES

- [1] MOMENI, A., ABBASI, S. M., BADRI, H. Hot deformation behavior and constitutive modeling of VCN200 low alloy steel. *Applied Mathematical Modelling*, 2012, vol. 36, no. 11, pp. 5624-5632.
- [2] OPĚLA, P., et al. Nový model pro predikci deformačních odporů oceli C45 za tepla. *Hutnické listy*, 2015, vol. 68, no. 6, pp. 53-59. (In Czech)
- [3] Gleeble Systems [online]. [viewed 2016-02-08]. Available from: <http://gleeble.com/products/mcu.html>
- [4] SCHINDLER, I., KAWULOK, P. Aplikáční možnosti plastometru Gleeble 3800 se simulačním modulem Hydrawedge II na VŠB-TU Ostrava. *Hutnické listy*, 2013, vol. 66, no. 4, pp. 85-90.
- [5] SCHINDLER, I., BOŘUTA, J. *Utilization Potentialities of the Torsion Plastometer*. Žory: OLDPRINT, 1998. 140 p.
- [6] ZENER, C., HOLLomon, J. H. Effect of Strain Rate Upon Plastic Flow of Steel. *Journal of Applied Physics*, 1944, vol. 15, no. 1, pp. 22-32.
- [7] KUBINA, T., et al. A new software calculating the activation energy. In *Forming 2005: 12th International Scientific Conference*. Ostrava: VŠB-TUO, 2005, pp. 145-150.
- [8] CINGARA, A., McQUEEN, H. J. New formula for calculating flow curves from high temperature constitutive data for 300 austenitic steels. *Journal of Materials Processing Technology*, 1992, vol. 36, no. 1, pp. 31-42.
- [9] Wei, Hai-lian, et al. Dynamic recrystallization behavior of a medium carbon vanadium microalloyed steel. *Materials Science and Engineering: A*, 2013, vol. 573, no. 20, pp. 215-221.
- [10] HENSEL, A., SPITTEL, T. *Kraft- und Arbeitsbedarf bildsamer Formgebungsverfahren*. 1<sup>st</sup> ed. Leipzig: Deutscher Verlag für Grundstoffindustrie, 1978. 528 p.
- [11] UNISTAT Statistics Software [online]. [viewed 2016-02-10]. Available from: <https://www.unistat.com/>
- [12] SHAFAT, M. A., et al. Prediction of hot compression flow curves of Ti-6Al-4V alloy in  $\alpha + \beta$  phase region. *Materials & Design*, 2011, vol. 32, no.10, pp. 4689-4695.